

## Multi-site optical excitation using ChR2 and micro-LED array

This article has been downloaded from IOPscience. Please scroll down to see the full text article.

2010 J. Neural Eng. 7 016004

(<http://iopscience.iop.org/1741-2552/7/1/016004>)

View [the table of contents for this issue](#), or go to the [journal homepage](#) for more

Download details:

IP Address: 147.46.117.211

The article was downloaded on 19/05/2010 at 07:37

Please note that [terms and conditions apply](#).

# Multi-site optical excitation using ChR2 and micro-LED array

Nir Grossman<sup>1,2</sup>, Vincent Poher<sup>3</sup>, Matthew S Grubb<sup>4</sup>,  
Gordon T Kennedy<sup>3</sup>, Konstantin Nikolic<sup>1</sup>, Brian McGovern<sup>1,5</sup>,  
Rolando Berlinguer Palmi<sup>1</sup>, Zheng Gong<sup>6</sup>, Emmanuel M Drakakis<sup>5</sup>,  
Mark A A Neil<sup>3</sup>, Martin D Dawson<sup>6</sup>, Juan Burrone<sup>4</sup> and  
Patrick Degenaar<sup>1,2</sup>

<sup>1</sup> Institute of Biomedical Engineering, Imperial College, London, UK

<sup>2</sup> Division of Neuroscience, Imperial College, London, UK

<sup>3</sup> Department of Physics, Imperial College, London, UK

<sup>4</sup> Department of Developmental Neurobiology, King's College, London, UK

<sup>5</sup> Department of Bioengineering, Imperial College, London, UK

<sup>6</sup> Institute of Photonics, University of Strathclyde, Glasgow, UK

E-mail: [nir.grossman@imperial.ac.uk](mailto:nir.grossman@imperial.ac.uk)

Received 29 July 2009


Accepted for publication 10 December 2009

Published 14 January 2010

Online at [stacks.iop.org/JNE/7/016004](http://stacks.iop.org/JNE/7/016004)

## Abstract

Studying neuronal processes such as synaptic summation, dendritic physiology and neural network dynamics requires complex spatiotemporal control over neuronal activities. The recent development of neural photosensitization tools, such as channelrhodopsin-2 (ChR2), offers new opportunities for non-invasive, flexible and cell-specific neuronal stimulation. Previously, complex spatiotemporal control of photosensitized neurons has been limited by the lack of appropriate optical devices which can provide 2D stimulation with sufficient irradiance. Here we present a simple and powerful solution that is based on an array of high-power micro light-emitting diodes (micro-LEDs) that can generate arbitrary optical excitation patterns on a neuronal sample with micrometre and millisecond resolution. We first describe the design and fabrication of the system and characterize its capabilities. We then demonstrate its capacity to elicit precise electrophysiological responses in cultured and slice neurons expressing ChR2.

 This article has associated online supplementary data files

(Some figures in this article are in colour only in the electronic version)

## 1. Introduction

The cognitive function of the brain is based upon coordinated activities of a large number of neuron cells. Coordination of activity in large-scale neural networks with single neuron resolution can enable the study of neural network dynamics [1] and cellular conditions which underlie pathological brain states, such as schizophrenia, epilepsy and other neuronal disorders [2]. Precise spatiotemporal control over large numbers of neurons is also required for clinical applications such as retinal prostheses.

Until recently, two-dimensional neural stimulation experiments have been based on micro electrode array (MEA) technology. The concept of MEA was first suggested by Thomas *et al* in 1972 [3] and since then it has been widely used in various neurological applications such as studying dynamics of neural networks [4], synaptic plasticity [5], visual perception [6] and effects of pharmacological compounds and putative therapeutics [7]. While MEAs have been successful at recording neural activity to high resolutions, stimulation is more challenging. The spatial resolution of the MEAs is limited and it does not allow targeting of individual neurons or dendritic compartments. Additionally, it can only

stimulate, not inhibit electrical activity. These limitations are fundamental to electrical stimulation: (a) stimuli are non-specific to particular cell types, (b) electrical pulses propagate through the solution and (c) fixed electrode locations [8]. Moreover, the MEA technique has an inherent ‘dead’ time between the stimulation pulse and the start of the recording due to the stimulation pulse saturating the signal. Apart from probing neural networks, two-dimensional stimulation is also required for investigation of the basic computation functions of individual neurons. Investigations include synaptic summation [9], spike-timing-dependent plasticity [10] and back-propagating action potential effects [11]. To perform such studies, a precise multi-site dendritic excitation that preserves physiological information flow from synapses to the soma is required. To date, precise spatiotemporal stimulation of the dendritic tree has been done with simultaneous dendritic and somatic patch pipette (e.g. [12]). These can provide very accurate recordings of the membrane voltages and currents, but the number of stimulation points is very limited. Therefore, there is a need for a device which can provide precise spatiotemporal stimulation of neuronal activity, both for neural network and single neuron experiments. The recent advances in molecular tools for photosensitization of neurons offer new opportunities. Light stimulation does not interfere with conventional recording techniques [13] and can be focused to sub-micrometre excitation spots with flexible location [14].

The concept of using light to stimulate neuronal signalling was first demonstrated in 1971 by Richard Fork from Bell laboratories [15]. Fork showed that action potentials can be generated in *Aplysia* ganglia by focusing high power blue (488 nm) laser light. While research in this area is ongoing with particular emphasis on auditory neurons [16], it requires extremely high irradiance. During the 1990s, neurostimulation based on photolysis of caged neurotransmitters such as caged glutamate was introduced [17] and has since been widely used. With this approach, spikes can be elicited with only 3 ms latency [18, 19]. Due to the ubiquitous presence of glutamate receptors in the CNS, photolytic uncaging of glutamate is a universal tool. The disadvantage of the ubiquitous presence of glutamate receptors is that activity is elicited in all neurons whose dendrites cross the uncaging beam [20]. In addition, prolonged experiments require continuous perfusion of the caged compounds. The spatial resolution of the technique can however be improved by attaching two caging groups [21] or using two-photon uncaging [18]. Recently, optical stimulation of neurons via attachment of light-activated agonists/antagonists [22] or pore blockers [23] into native ion channels has been shown. However, it requires both genetic modification of native channels and a chemical attachment of light-activated photo-conformable units. In addition, UV light has been associated with DNA damage [24]; hence photostimulation techniques which require UV illumination are generally undesirable and unlikely to be used in the future for neural prosthesis applications.

In 2003, a new era in optical stimulation of neurons started with the discovery of the light-sensitive ion channel, channelrhodopsin-2 (ChR2) [25]. This was followed up by the rediscovery of the optically activated chloride pump,

halorhodopsin [26]. These can be genetically expressed in neurons and the field has thus been termed ‘*optogenetics*’. ChR2 is a non-selective light-sensitive cation channel (in fact it is bifunctional, a proton pump with a leak that shows ion channel properties [27]) with an action-spectrum peak at around  $\sim 460$  nm [25]. Since the demonstration by Boyden *et al* [28] of millisecond spiking control in hippocampal neurons, the functionality of ChR2 has been demonstrated in numerous neurons *in vitro* [29–33] and *in vivo*: *Caenorhabditis elegans* [34, 35], mouse retina and brain [36–45], *Drosophila* [46–49], rat [50–52] and recently also in nonhuman primates [53]. ChR2 has provided a powerful tool for fast excitation of neural activities with visible light. However, the high irradiance requirements of ChR2 have hindered the development of methods for two-dimensional spatiotemporal control. The minimum spiking irradiance of ChR2 using 470 nm light is between 0.1 and 1 mW mm<sup>-2</sup> (corresponding to the minimum light source luminance of 10<sup>6</sup>–10<sup>7</sup> cd m<sup>-2</sup>) [8, 54]. This level of irradiance can be achieved with high power light sources such as arc lamps [28, 55], lasers [14, 38, 44, 53, 56] and bulk high power light-emitting diodes (LEDs) [13, 41, 57, 58]. However, these light sources are limited to whole-field or single focused point illuminations and hence lack patterning capacity. Conventional two-dimensional structured light sources, such as back-lit liquid crystal displays (LCDs), plasma screens and organic light-emitting diodes (OLEDs) displays have the capacity to achieve good spatial resolution, but lack the illumination strength. Typical displays in this class can generate irradiance in the range of  $0.25 \times 10^{-4}$ – $1 \times 10^{-4}$  mW mm<sup>-2</sup> (250–1000 cd m<sup>-2</sup>). They are thus three orders of magnitude too dim to effectively excite ChR2. Moreover, the frame rates of high power liquid crystal devices are typically limited to around 100 Hz.

In principle, patterned excitation can be achieved by scanning a single high power light source such as a laser, by using for example fast beam modulators such as acousto-optical deflectors or galvanometric devices. This principle has been demonstrated on photolysis of caged glutamates in two dimensions [18] and even three dimensions [59]. Yet, although the point-to-point travelling time of the laser beam can be very fast (tens of microseconds), the number of neural locations that can be synchronized is limited. For example, synchronizing 100 neuronal locations with a 10  $\mu$ s light pulse and 10  $\mu$ s point-to-point travelling time introduces almost 2 ms delay between the excitation of the first and the last neuronal location (which is in the time scale of a complete action potential). In practice, the scanning speed is limited by prolonged illumination time at each stimulation point that is required for evoking action potentials (for example, Nikolenko *et al* [60] reported minimum illumination per cell of 5 ms). Hence, it may be impractical in applications involving simultaneous stimulation of large numbers of neuronal targets.

Previously, we showed [61] that stripe arrays of gallium nitride micro-LEDs could provide sufficient irradiance to induce photolysis of caged fluorescein and evoke spikes in ChR2-expressing neurons. However, since each LED stripe was 17  $\mu$ m wide and 3600  $\mu$ m long, it could not localize

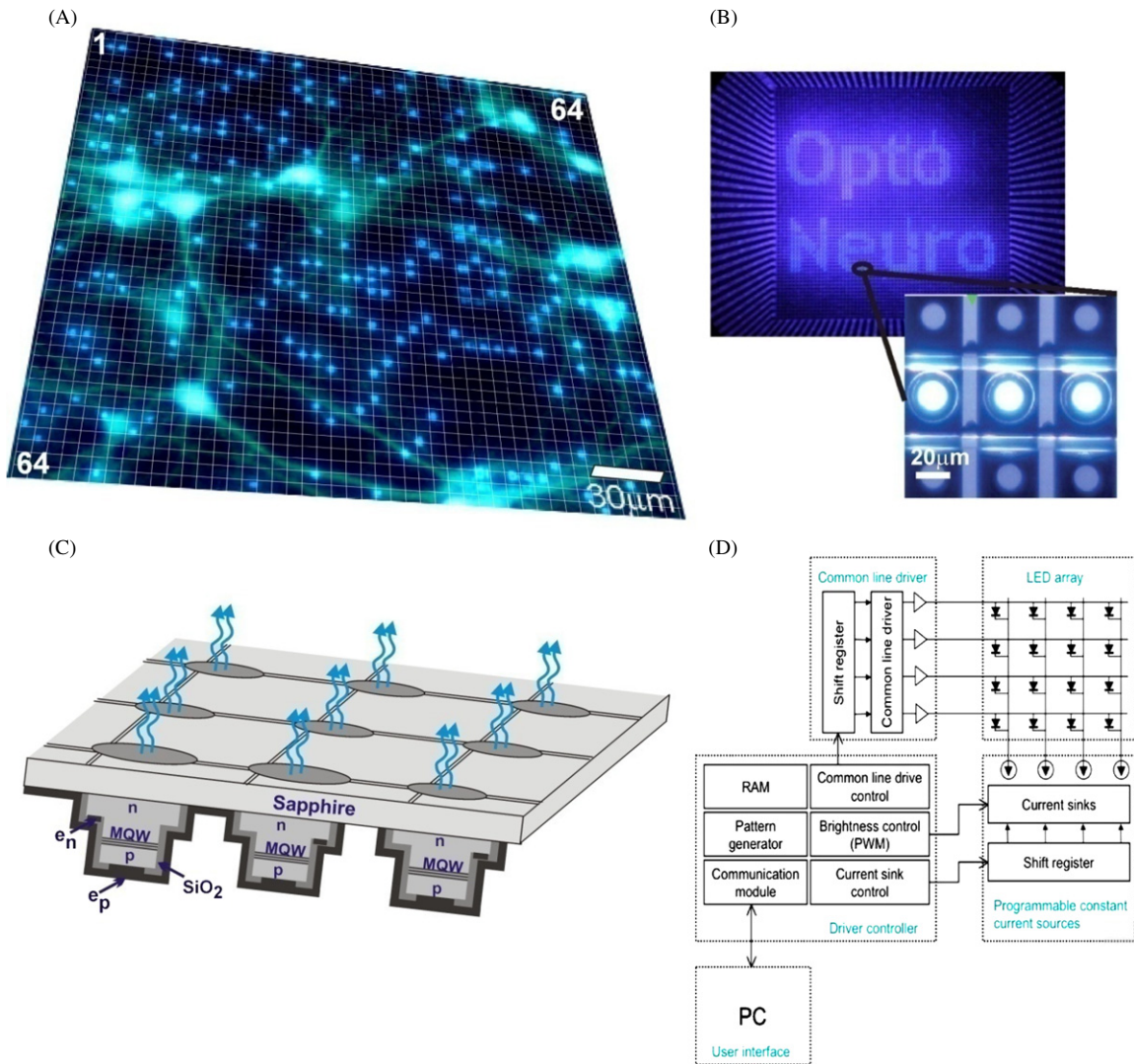


**Figure 1.** Concept of matrix photostimulation. (A) Neural cells expressing Chr2 are covered by the 64 × 64 matrix of bright small light spots, with individual control of their intensity and timing. (B) The micro-LED array. (C) Illustration of the micro-LED structure showing the different micro-layers. n: n-type GaN; p: p-type GaN; MQW: multiple quantum wells; SiO<sub>2</sub>: silicon dioxide; e<sub>n</sub>: n-contact; e<sub>p</sub>: p-contact. (D) Schematic of the matrix-addressed control circuit.

illumination to individual neurons or sections of the dendritic tree. Here, we present a solution based on a matrix of micro-LEDs, which is a two-dimensional high-power micro-LED array (MLA) that can generate arbitrary excitation patterns (figures 1(A) and (B)) with micrometre and sub-millisecond resolutions and sufficient irradiance to generate Chr2-evoked spiking in neurons. We demonstrate the capability of the system to elicit precise electrophysiological responses in Chr2-expressing neurons and show examples of potential uses of the photonic matrix. Finally, we discuss the limitations of the technique relative to other potential technologies.

## 2. Materials and methods

### 2.1. Micro-LED design and fabrication

64 × 64 arrays of 20 μm diameter micro-emitters with 50 μm centre-to-centre spacing (figure 1(B)) were fabricated by processing gallium nitride semiconductor wafers into

micro-structured arrays of emitters. A detailed description of the fabrication procedure can be found in [62, 63] and is summarized below. A schematic illustration of the micro-LED array structure is shown in figure 1(C). The wafers consist of a sapphire substrate, a few microns thick Si-doped GaN (n-substrate), three InGaN/GaN quantum wells and 0.25 μm of Mg-doped GaN (p-substrate). The emission spectrum depends on the material band gap and can be tuned from violet to amber by changing the relative fraction of InGaN in the InGaN/GaN quantum wells [64, 65]. The structure was annealed at 980 °C for 10 s in nitrogen ambient to activate Mg acceptors. Then, isolated columns with a common cathode were formed using Cl<sub>2</sub>/Ar inductively coupled plasma (ICP) dry etching through the complete LED structure (including the n-substrate). Next, individual LEDs were formed by a second dry etching stage (down to the n-substrate) to form isolated anodes. The inter LED gaps were filled with non-conductive plasma-enhanced chemical vapour deposition

(PECVD) SiO<sub>2</sub>. In the next stage, the structure was polished via chemical mechanical planarization (CMP) using 0.1 mm SiO<sub>2</sub> particles in a KOH solution with a pH of 10. Finally, n-type Ti/Pt/Au and reflective p-type Ni/Au/Ti/Au ohmic contacts were deposited using e-beam metal evaporation and were thermally annealed at 600 °C for 5 min in nitrogen ambient.

## 2.2. Electronic control system

The micro-LEDs are addressed in a matrix fashion [66] in which a single emitter is controlled by applying a positive bias voltage across its row electrode and sinking a constant current from its column electrode. A schematic of the control system is shown in figure 1(D). The bias voltages are generated by eight serially connected MIC5891 (Micrel Semiconductors) programmable high voltage drivers. Each driver has eight open emitter outputs, each capable of sourcing 500 mA at up to 35 V. The columns are connected to four serially connected constant current sink drivers MAX6971 (Maxim). The MAX6971 has 16 current outputs, which are able to sink from 3 mA to 55 mA per output. The drive current is adjusted through an external quad 256-step digital potentiometer controlled by a peripheral interface controller PIC18F4550 (Microchip) working at 48 MHz. The PIC18F4550 connects to a computer via the USB port and receives user inputs via a virtual RS-232 serial port. On start-up, the PIC continuously polls whether data have been sent from the host computer. Received data are stored in memory in the PIC microchip and then parsed to extract and implement user commands. The brightness of the LEDs can be modulated by changing the current sinks or through pulse width modulation (PWM) under the control of the microcontroller. In the PWM approach, the current-sinking outputs in the MAX6971 device are enabled periodically and the brightness is tuned by changing the duty cycle (i.e. the ratio of the on pulse duration to the flashing period). The array is turned on and off when the processor receives 1-byte ('+' and '-') command. Programmable timers in the PIC can be used to implement pulse trains with microsecond timing accuracy. The control of the PIC18F4550 is carried out by a PC via Matlab (MathWorks Inc.)-based control interface, utilizing the data acquisition toolbox 8.1.

## 2.3. Microscope setup

We used an Olympus IX71 inverted microscope equipped with a 40× oil-immersion objective (NA = 1.00). In order to localize and target fluorescent ChR2-expressing neurons, we used a xenon arc lamp (Lambda LS; Sutter) where the light is regulated by a rapid shutter (smartShutter, Sutter Instrument) driven by a Sutter Instruments Lambda 10–3 controller and fitted with a 470 ± 20 nm bandpass excitation filter (Chroma Tech). The setup was also tested on a Nikon Eclipse 2000 microscope.

## 2.4. Optical characterization

The emission spectrum of the matrix was measured by placing a USB2000 spectrometer (Ocean Optics) directly above the

emitters. In order to measure the currents through the emitters and the corresponding emission powers, the micro-LED chip was placed on an isolated mount so that currents could be injected directly through individual LEDs. We used a Keithley 2000 multimeter (Keithley Instruments Inc.) to inject the currents and a Fluke 73111 (Fluke Ltd) voltmeter and a FieldMaxII-TO (Coherent) power meter to measure the voltage and emission power, respectively. The power meter was placed on the micro-LED chip. Variability in the emission power was tested by driving the micro-LEDs one-by-one and monitoring their emission powers using the same power meter. Characterization of on-sample illuminations was carried out by projecting the micro-LEDs onto a 5 mm thick glass slide with a specially deposited 90 nm thin fluorescent coating. The illumination spots were imaged using a CCD camera (MicroPublisher 3.3 RTV *QImaging* with 2048 × 1536 pixels and 3.45 μm × 3.45 μm pixel size) and analysed with Origin (Origin Lab). The on-sample emission powers were measured by placing the power meter FieldMaxII-TO on the sample plane.

## 2.5. Hippocampal neurons culture and transfection

Primary dissociated cultures were obtained from hippocampal tissue of Sprague-Dawley rats on embryonic day 18.5. Hippocampi were digested in trypsin (1 mg ml<sup>-1</sup> in HBSS, 15 min at 37 °C) and dissociated in neurobasal medium with 10% FCS by passing through a series of decreasing diameter Pasteur pipettes. They were then plated at 300 cells mm<sup>-2</sup> on 18 mm diameter, thickness no. 1 glass coverslips (Glaswarenfabrik Karl Hecht) coated with 50 μg ml<sup>-1</sup> poly-D-lysine (PDL) and 20 μg ml<sup>-1</sup> laminin. Cultures were grown in neurobasal medium supplemented with 10% FCS, 0.5% penstrep and 1× glutamax for the first 2 h *in vitro*, and thereafter in neurobasal medium with B27, 0.5% penstrep and 1× glutamax at 37 °C and 6% CO<sub>2</sub>. The neurons were transfected at 7 days *in vitro* (DIV) using a lipofectamine procedure with a fusion ChR2–YFP (a gift from Karl Deisseroth, Stanford) that was subcloned into a plasmid containing a chick β-actin promoter.

## 2.6. Patch clamp recording of hippocampal neurons

Electrophysiological recordings were performed at 10–14 DIV. Although the cells can also be patched in a later stage, we found that in this time window the neurons were morphologically well developed with the established synaptic network as well as young enough to enable efficient whole-cell recordings. The electrophysiological responses were obtained using patch clamp methods to measure the effect of optical stimulation. Individual coverslips were placed in a custom recording chamber and bathed with room-temperature HEPES-buffered saline (HBS) containing, in mM, 136 NaCl, 2.5 KCl, 10 HEPES, 10 D-glucose, 2 CaCl<sub>2</sub>, 1.3 MgCl<sub>2</sub>, 0.01 gabazine, 0.01 NBQX and 0.025 APV (285 mOsm, pH 7.4). Patch pipettes, pulled from borosilicate glass (1.5 mm OD, 1 mm ID, 3–4 M), were filled with a solution containing, in mM, 130 K-gluconate or Cs-gluconate, 10 NaCl, 1 EGTA, 0.133 CaCl<sub>2</sub>, 2 MgCl<sub>2</sub>,

10 HEPES, 3.5 Na-ATP and 1 Na-GTP (280 mOsm, pH 7.4). Conventional whole-cell patch-clamp recordings were obtained via a Heka EPC10 double patch amplifier coupled to Pulse acquisition software. Signals were sampled at intervals of 65–150  $\mu\text{s}$  (6.7–15.4 kHz) and were low-pass filtered using a four-pole Bessel filter at 2.9 kHz (filter 2). The holding potential in voltage-clamp mode was  $-70$  mV using 0 pA holding currents, uncorrected for any liquid junction potential (probably in the range of +10 mV) between our internal and external solutions. The cells had a mean input resistance of ( $\pm$ SEM)  $573 \pm 116$  M $\Omega$  (nine cells).

### 2.7. *rd1* mice transfection

Retinas of *rd1* knock-out mice that lose their photoreceptors by 4 weeks of age were transfected with ChR2 and stimulated using the micro-LED array. C3H/HeNcr1 (*rd1*) mice were purchased from Charles River Laboratories (L'Arbresle Cedex, France). The animals were maintained under a 12 h light–dark cycle and at  $1.6 \times 10^{13}$  photons  $\text{cm}^{-2} \text{s}^{-1}$  (between 400 and 500 nm) illumination during the daytime. At 4–5 weeks after birth, the right eyes of the mice were injected with pAAV-double floxed-hChR2 (H134R)-mCherry-WPRE-pA (a gift from Karl Deisseroth, Stanford). The *rd1* experiments were done with Boton Roska at Friedrich Miescher Institute for Biomedical Research, Basel. All animal procedures were performed in accordance with the standard ethical guidelines (European Communities Guidelines on the Care and Use of Laboratory Animals: 86/609/EEC) and were approved by the Veterinary Department of the Canton of Basel-Stadt.

### 2.8. Multi-electrode array recording of *rd1* retina

To record extracellular voltage transients in the retinal preparations, we used a MEA. Isolated retinas of *rd1* mouse were placed on a flat MEA60 200 Pt GND array (*Ayanda Biosystems*). The 30  $\mu\text{m}$  diameter microelectrodes were spaced 200  $\mu\text{m}$  apart on the array. The retina was continuously superfused in oxygenated Ringer's solution (110 mM NaCl, 2.5 mM KCl, 1.0 mM  $\text{CaCl}_2$ , 1.6 mM  $\text{MgCl}_2$ , 22 mM  $\text{NaHCO}_3$ , 10 mM D-glucose (pH 7.4 with 95%  $\text{O}_2$  and 5%  $\text{CO}_2$ )) at 36 °C during experiments. The signals were recorded with MEA1060-2-BC (Multi-Channel Systems) and filtered between 500 Hz (low cut-off) and 3500 Hz (high cut-off). The spikes were extracted with a threshold of four times the standard deviation of the recorded trace using Matlab code (MathWorks).

## 3. Results

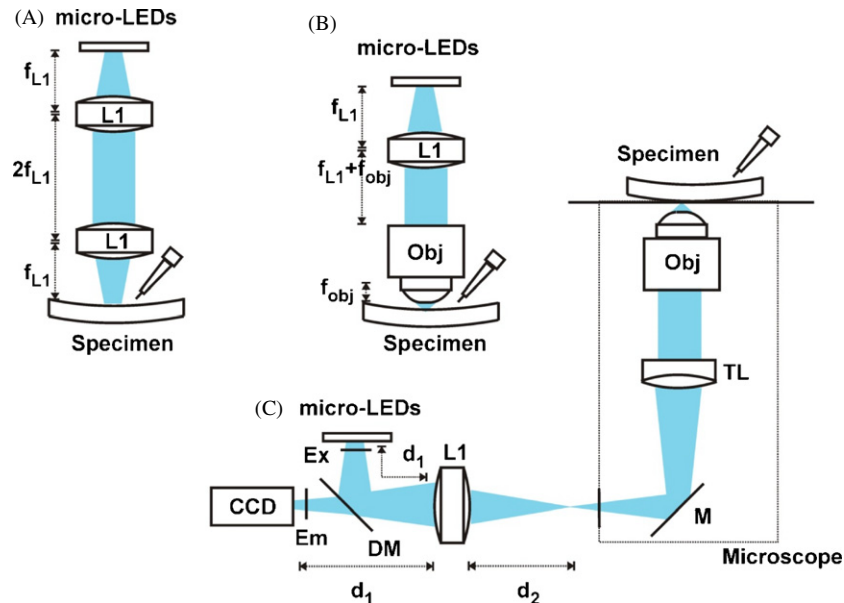
### 3.1. System design and characterization

The photonic matrix (shown in figure 1(B)) is a  $4 \times 4$  mm<sup>2</sup> chip consisting of a  $64 \times 64$  matrix of 20  $\mu\text{m}$  diameter micro-LEDs with 50  $\mu\text{m}$  centre-to-centre spacing. Each micro-LED is individually controlled and can be switched on/off with millisecond resolution. The emission spectrum of the micro-LEDs is centered at 470 nm with a 22 nm

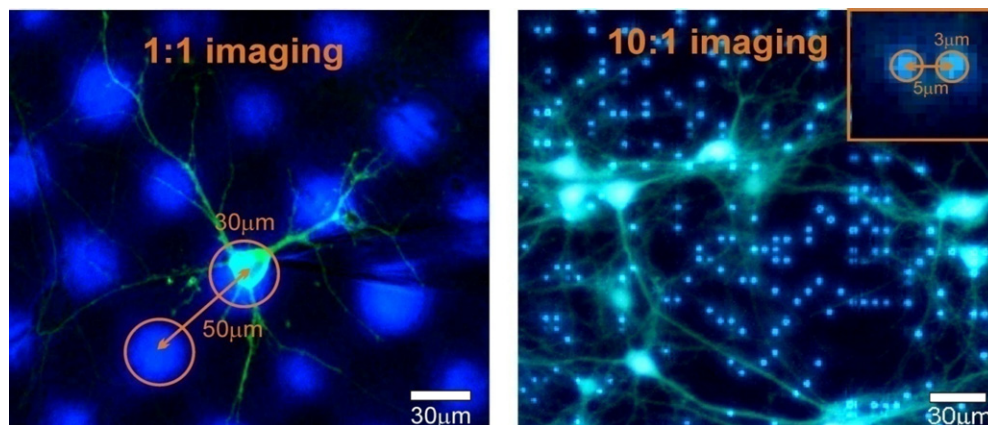
FWHM (full width half maximum) and hence overlaps with the peak sensitivity of ChR2 (see figure 4(A)). Each micro-LED can operate with high current densities to provide an output emission power of 70  $\mu\text{W}$ , corresponding to an on-emitter irradiance of 250  $\text{mW mm}^{-2}$ , enough light to surpass the ChR2 stimulation threshold. Two optical configurations were designed to image the photonic matrix onto the neuronal sample (figure 2). The first configuration (shown in figure 2(A)) images the micro-LEDs with their original size (1:1 imaging) and was designed for stimulation of neural networks. The photonic matrix generated a stimulation field of  $3 \times 3$  mm<sup>2</sup> in which a single-cell soma can be covered by one light spot (figure 3, left). The design consisted of two S5LPJ2851 (Sill Optics GmbH) AR (anti-reflective) coated 50 mm NA = 0.14 triplet lenses, i.e. consists of three single lenses, arranged in a  $4f$  relay configuration (figure 2(A)). It had a large focal length which allowed long (40 mm) working distance that was sufficient to accommodate electrophysiology recording apparatus such as a patch clamp or MEA. The use of triplet lens elements helped to minimize the spherical aberration. Although the system was not diffraction limited, the peak to valley aberrations were less than 1.5 wavelengths across the entire field. The on-sample spots had a FWHM size of 30  $\mu\text{m}$  and a 50  $\mu\text{m}$  centre-to-centre spacing (figure 4(B)). This configuration had however low collection efficiency ( $\sim 2\%$ ) due to the small input NA (in the case of a small Lambertian source the collection efficiency  $\eta$  of a lens having a numerical aperture NA is given by  $\eta \approx \text{NA}^2$ ). Typically, the working distance of the system is determined by the output NA (small NA enables large working distance) and the collection efficiency is determined by the input NA (large NA enables high collection efficiency); the choice of lenses is a trade-off between light collection efficiency and working distance. Nevertheless, the on-sample irradiance from a single emitter, driven by 8 mA current at 7 V, was  $3 \pm 0.2$   $\text{mW mm}^{-2}$  (figure 4(C)) which is above ChR2 spiking threshold. The illumination of the micro-LED was stable and changed by only 3% (i.e. maximum irradiance change of 0.03  $\text{mW mm}^{-2}$ ) during 1 h of continuous illumination. The illumination spots were relatively homogeneous with on-spot power fluctuation of less than 20%, figure 4(B).

The second optical configuration (shown in figure 2(B)) de-magnifies the micro-LEDs by approximately a factor of 10 (10:1 imaging) and was designed for detailed examination of a single neuron or a small-scale neural network. The design consisted of one S5LPJ2851 (Sill Optics GmbH) 50 mm triplet lens and one LUMPlanFI 40 $\times$  water immersion objective (Olympus) with 4.5 mm focal length and NA = 0.8. In this case, the photonic matrix generated a stimulation field of  $0.3 \times 0.3$  mm<sup>2</sup> in which each spot had a FWHM size of  $\sim 3$   $\mu\text{m}$  and a centre-to-centre spacing of  $\sim 5$   $\mu\text{m}$  (figure 3, right). The on-sample irradiance from a single emitter driven by 8 mA current at 7 V was  $\sim 300 \pm 20$   $\text{mW mm}^{-2}$ , figure 4(C). The on-sample illumination had a fill factor of  $\sim 16\%$ . The fill factor can be improved by introducing a micro-lens array, as is discussed later.

The micro-LEDs can also be projected on the sample via the microscope camera/epi-fluorescence illumination port. A design for illumination via the camera port is shown in



**Figure 2.** Imaging configurations. (A) Micro-LED matrix is imaged 1:1 on the neural sample using two lenses in  $4f$  relay configuration. (B) Optical setup for 10:1 imaging using one lens and an objective. (C) Optical setup to couple the micro-LED matrix to a microscope via the camera port. L1, lens (we used S5LPJ2851 (Sill Optics GmbH) 50 mm triplet); Obj, objective (we used LUMPlanFI (Olympus)  $40\times$  water immersion objective);  $f_{L1}$ , focal length of L1 (50 mm);  $f_{obj}$ , focal length of Obj (4.5 mm);  $d_1$  and  $d_2$ , object and image distance (e.g.  $d_1 = d_2 = 2f_{L1} = 100$  mm), Ex and Em, excitation and emission filters; DM, dichroic mirror (e.g. FITC filter block 41001 (Chroma), Ex: 480 nm, Dichroic: 505 nm, Em: 535 nm); M, mirror; TL, tube lens.



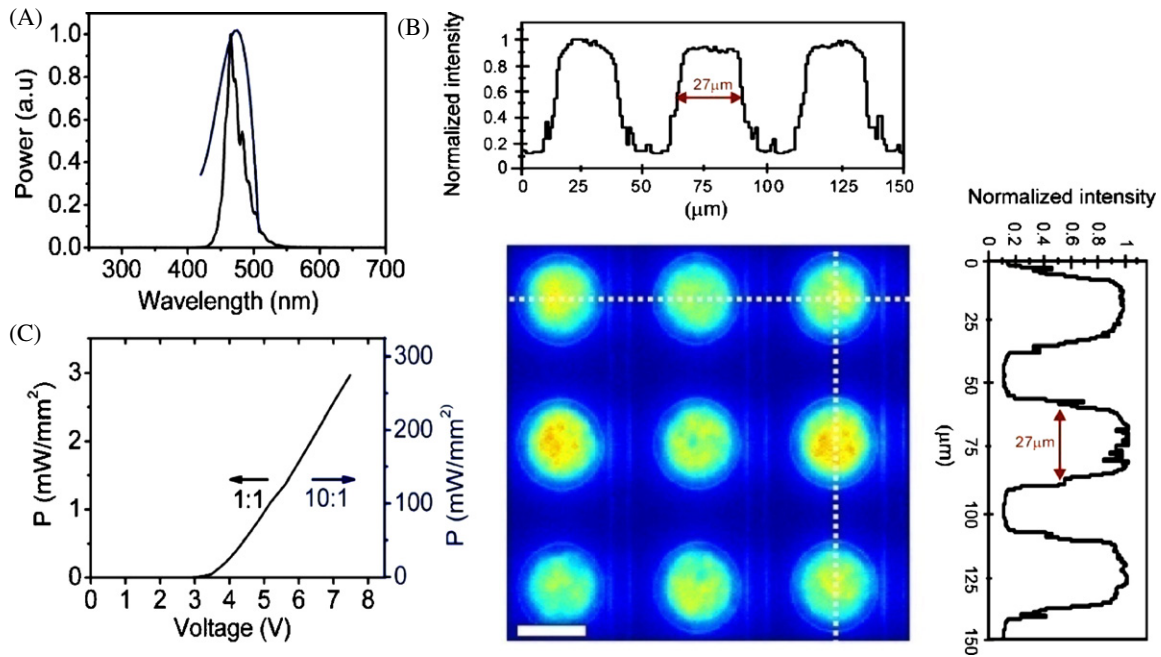
**Figure 3.** On-sample illumination. Left: a brightfield image of micro-LEDs projected onto neural sample using the 1:1 optic configuration. Right: an overlay image of the micro-LEDs projected using the 10:1 configuration. Inset: zoomed view. The overlay is a combination of a brightfield micro-LED illumination and a fluorescence imaging of the YFP tag expressed in the neurons with the Chr2.

figure 2(C). In this case, the microscope tube lens and objective image the micro-emitters onto the sample; in the same way the sample is imaged onto the microscope camera. The size of the illumination spots is determined by the objective. The array is projected onto an  $L/M \times W/M$  mm<sup>2</sup> image at the sample plane, where  $M$  is the objective magnification and  $W$  and  $L$  are the width and length of the matrix, respectively. When the micro-LEDs and the CCD camera share the same port, a dichroic mirror and a single lens can be used to couple the two to the microscope port as shown in figure 2(C). In this case, due to the high brightness of the micro-LEDs, filters are typically required to eliminate the saturation of the camera by LED light that is reflected by the lenses. Using the epi-illumination port can be more complicated since the epi-illumination path is typically designed for Köhler principle [67] imaging as both

the field lens and the diaphragm are typically integrated in the microscope and hence imaging the matrix via the epi-port can require adjustments or removal of internal microscope lenses.

### 3.2. Spike generation and temporal resolution

First, we tested if the spot generated by a single micro-emitter that is imaged 1:1 has sufficient irradiance to elicit action potentials in Chr2-expressing neurons. The micro-LEDs were mounted above the microscope stage as in the configuration shown in figure 2(A) using a mechanical arm with a 25 mm XYZ actuator (Thorlabs). The image of the photonic matrix was located at the centre of the field of view (FOV) and brought to focus on the sample plane using the XYZ actuator and a visual feedback from the eyepiece or camera. Then, fine



**Figure 4.** Characteristics of on-sample illumination. (A) Normalized emission spectrum of the micro-LEDs (black) plotted together with the action spectrum of ChR2 (estimated from [25]). (B) Intensity map of  $3 \times 3$  micro-LEDs presented with graphic view of the intensity profile along the white lines. Scale bar =  $25 \mu\text{m}$ . (C) On-sample irradiance from a single emitter as a function of the bias voltage. Left vertical axis: 1:1 imaging; right vertical axis: 10:1 imaging (note: curves overlaid).

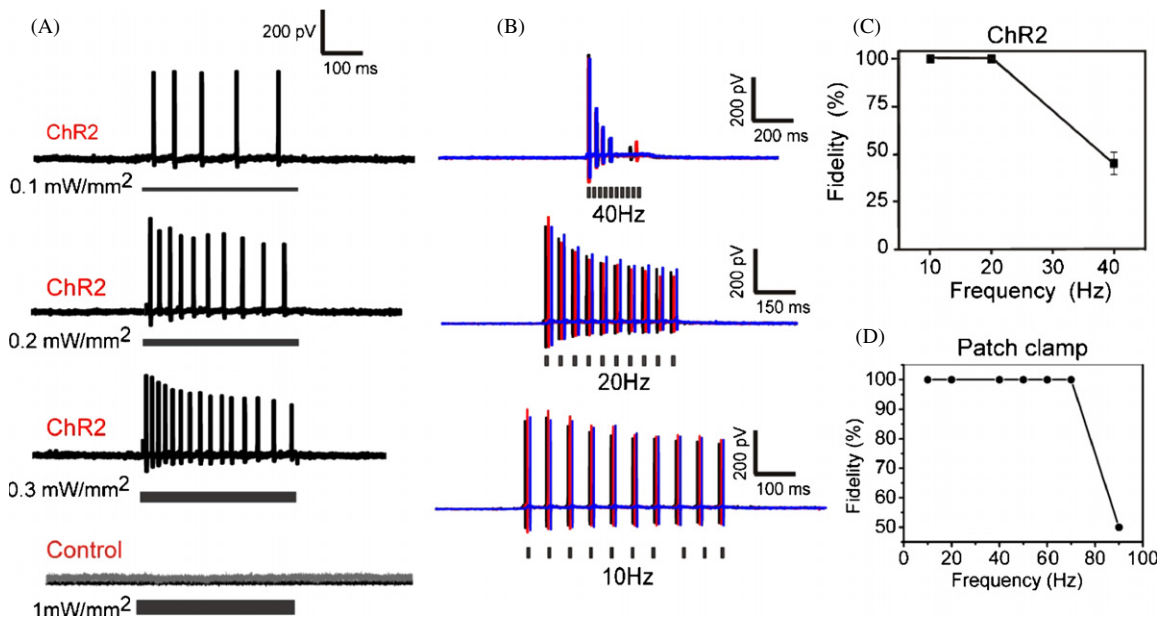


**Figure 5.** Spike generation and temporal resolution. (A) Continuous stimulation. From top to bottom, illumination of ChR2-expressing neurons using 1:1 imaging with 500 ms pulses at on-sample irradiances of  $0.1 \text{ mW mm}^{-2}$ ,  $0.2 \text{ mW mm}^{-2}$  and  $0.3 \text{ mW mm}^{-2}$ . Bottom: illumination of non-transfected neurons with 500 ms pulse of  $1 \text{ mW mm}^{-2}$  ( $n = 3$ ). (B) Pulse stimulation. From top to bottom, illumination of ChR2-expressing neurons using 1:1 imaging with 40 Hz, 20 Hz and 10 Hz trains of 5 ms  $1 \text{ mW mm}^{-2}$  light pulses. The results show overlap of three recordings (coloured blue, red and black) (C) Summary of spiking fidelity versus stimulation frequency using the 1:1 imaging setup. (D) Spiking fidelity versus frequency using pulses of 200 pA current injection stimulation.

tuning was carried out to ensure that a single spot was aligned on a soma of a ChR2–YFP-expressing neuron. Localization of the neuron was carried out via fluorescence imaging. The cells were then illuminated with a continuous 500 ms pulse and their electrophysiological responses were recorded using a patch clamp apparatus in the cell-attached configuration. When

illuminated, the neurons fired spike trains with a frequency adaptation feature (higher frequency at the beginning), figure 5(A). The spiking terminated when the light was turned off. We found that the steady-state spiking frequency was between 0 and 15 Hz and was proportional to the emission power (data not shown). No spiking response was recorded



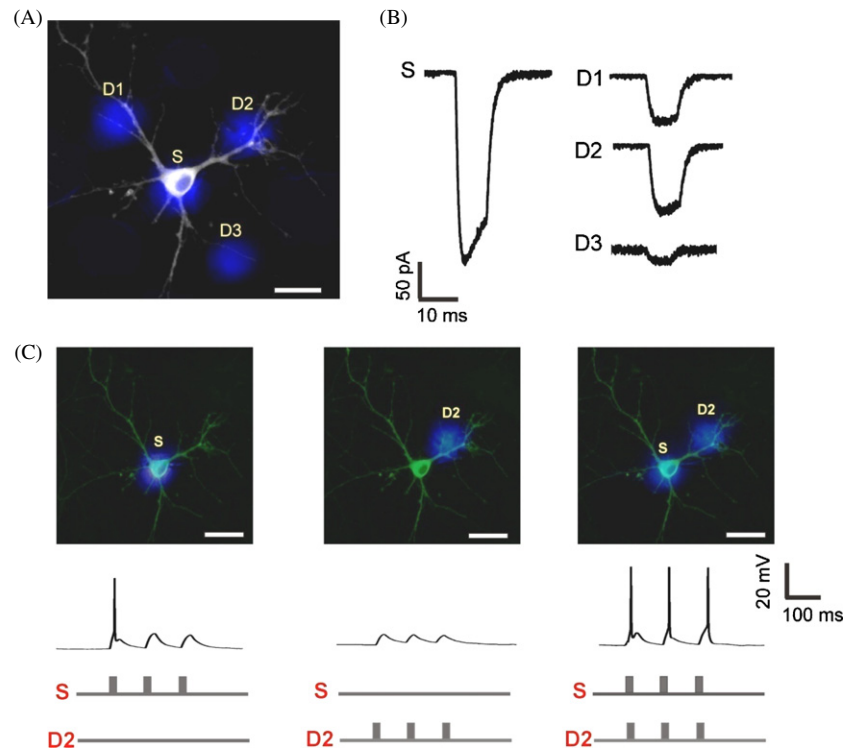


**Figure 6.** Dendritic excitation. (A) Illumination (1:1) of three proximal dendrites and cell soma of ChR2-expressing hippocampal neuron. (B) Currents evoked by 10 ms of  $1 \text{ mW mm}^{-2}$  illumination. (C) ChR2-evoked input currents were synchronized to maximize spiking output. Scale bar is  $30 \mu\text{m}$ .

in non-transfected neurons (figure 5(A), ‘control’), indicating that the irradiance alone does not elicit response.

Next, we examined the efficiency of the micro-LEDs to drive precisely timed action potentials. The cells were illuminated using the same 1:1 imaging configuration with trains of short (5 ms) light pulses at different frequencies. The responses were recorded again using a patch clamp apparatus in the cell-attached configuration. The results, shown in figure 5(B) and summarized in figure 5(C), indicate that the micro-LEDs could reliably elicit optically controlled action potentials. At high frequencies (higher than 20 Hz), the fidelity of the stimulation, i.e. the percentage of successful light evoked spikes, dropped. In comparison, when the neurons were stimulated by injection of 200 pA currents via the patch clamp apparatus, we obtained high fidelity between stimulation and recorded action potentials up to frequencies of 70 Hz (cultured hippocampal neurons can normally spike up to 100 Hz [68]). The loss of efficiency for ChR2-transfected cells at high frequencies is not a unique feature of the micro-LED illumination or hippocampal cells and has been widely reported in the literature for other light sources and biological models, for example, Boyden *et al* 30 Hz [28], Li *et al* 5 Hz [29], Ishizuka *et al* 20 Hz [30], Arenkiel *et al* [43] and Wang *et al* 40 Hz [42] and Zhang *et al* 50 Hz [55]. The fidelity is a function of ChR2 expression and the fundamental biophysics of the ChR2. Higher levels of expression can lead to stronger evoked currents and hence improved spiking fidelity. Also, while the fidelity is independent of the type of illumination, it is improved with higher levels of illumination, as discussed later.

### 3.3. Example of dendrite excitation

Next, we wanted to test if the photonic matrix can generate sufficient dendritic currents that can be used in a single neuron computation. The micro-LED matrix was imaged on the neurons using the 1:1 imaging configuration and its location was adjusted so that a single spot was centred on the soma of a CHR-YFP-encoded neuron. Then the central spot and the spots adjacent to the central one, see figure 6(A), were turned on one by one for 10 ms ( $1 \text{ mW mm}^{-2}$ ) and their electrophysiological responses were recorded with a whole-cell voltage clamp at  $-70 \text{ mV}$  using  $0 \text{ pA}$  holding currents. The results, shown in figure 6(B), indicate that notable currents of up to  $60 \text{ pA}$  were stimulated by illuminating the dendrites. We then tested if the neuron can integrate these dendritic inputs with the larger somatic currents. For that reason, we illuminated the soma and a proximal dendrite, first separately and then synchronously, with short trains of 10 ms ( $1 \text{ mW mm}^{-2}$ ) light pulses repeated at 10 Hz, and recorded the neuronal depolarization responses using a whole cell current clamp. The results presented in figure 6(C) show that the currents evoked in the soma were sufficient to generate only the initial action potential and were not sufficient to sustain further spiking. In contrast, when the somatic stimulation was synchronized with the dendritic one, it was sufficient to sustain a complete spike train. This simple experiment illustrates in fact the capacity of the neuron to integrate and fire from multiple compartments as was first suggested by Lapicque [69].

We also examined briefly the differences in the way these dendrites conduct the input stimuli to the soma. Given that

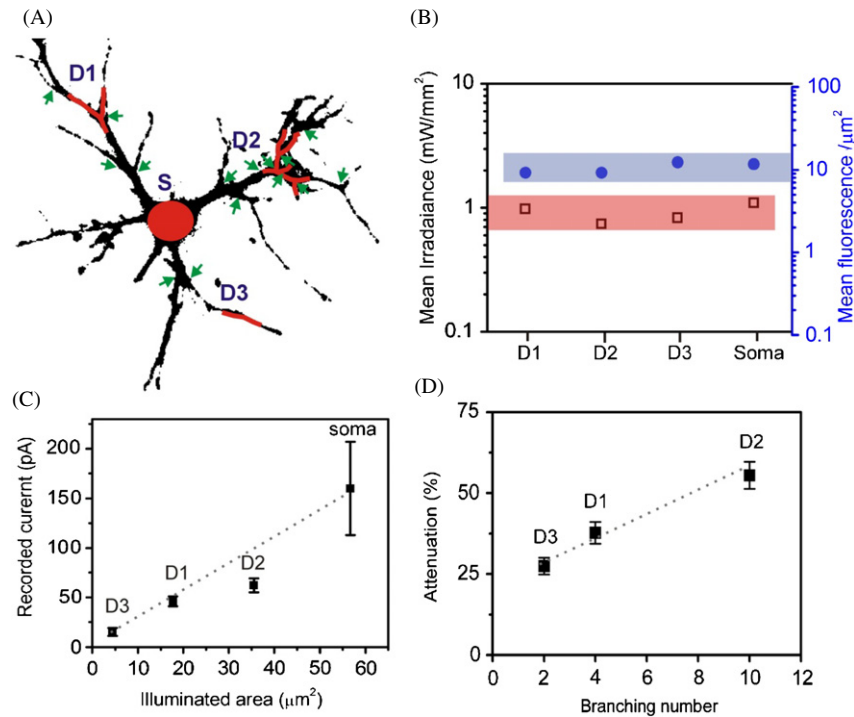


**Figure 7.** Probing dendritic conductance. (A) Illustration of the neuron (black) with the stimulation locations (grey/red) and the dendrites branching (green arrows) highlighted. (B) Mean irradiance (red) and mean fluorescence density (blue) at the excitation sites. (C) Evoked currents recorded at the soma versus the area of illumination at the excitation sites. (D) Attenuation of the dendritic signals versus the number of dendritic branching ( $n = 3$ ).

the dendrites were excited at similar distances (relatively close  $35 \mu\text{m} \pm 2 \mu\text{m}$ ) from the soma, we assumed that there would be relatively small differences in the level of the passive voltage attenuations. As ChR2 was co-expressed with YFP, the relative densities of expression can be determined via the fluorescence profile (images were recorded under whole-field epi-illumination from a xenon lamp using a CCD camera). Figure 7(B) shows that the ChR2 density was similar across the illuminated spots, as was the irradiance profile. In this case, we expected that the evoked currents that were recorded at the soma would be proportional to the size of the illuminated area. The illumination areas are illustrated in grey (red) in figure 7(A), and the recorded currents versus the illuminated areas are plotted in figure 7(C). The plot implies that the currents recorded from D2 were lower than expected from the area analysis. In principle, the currents recorded at the soma were affected by both current leakage via dendritic branching [70] and fluctuation in the membrane potentials which are associated with the space clamp problem [71]. We expected that since the excitations were done in proximal dendrites and the voltage clamp recording used 0 pA holding currents, the space clamp errors might have been small in this case. Indeed, we observed a linear relationship between the level of attenuation and the number of branches (marked with (green) arrows in figure 7(A)) from the input sites (adjacent branching on the distal side of the inputs was included as well since it could have ‘sink’ currents) as shown in figure 7(D). It should be noted that although the results imply the level of attenuation linearly proportional to the number of branches, our calculations did not take into

consideration possible differences in the width of the dendrites and/or branching—a wide branch point might attenuate more than a certain number of small branch points (it all depends on the relative ratios of the daughter branch diameters).

### 3.4. Example of tissue stimulation

During the last decade, there have been immense efforts worldwide to develop retinal prostheses for patients suffering from degenerative retina diseases such as retinitis pigmentosa [72, 73]. Recently, a new type of retinal prosthesis that uses ChR2 to render light sensitivity onto the residual retinal neurons has been suggested [8, 40, 45, 52]. ChR2-based retinal prostheses require however a light source that is capable of generating two-dimensional stimulation patterns (resolution  $> 1000$  points) with micrometre ( $\leq 20 \mu\text{m}$ ) and millisecond ( $< 1$  ms) resolution and with sufficient radiance ( $> 50 \text{ mW mm}^{-2} \text{ sr}^{-1}$ ) to induce action potentials in neurons [8]. The photonic matrix provides a compact and powerful solution ideal for future head-mounted devices. Each emitter has sufficient radiance of  $210 \text{ mW mm}^{-2} \text{ sr}^{-1}$  (it emits  $70 \mu\text{W}$  light into a solid angle of  $2\pi$  steradians and the emission area is  $\sim 3 \times 10^{-4} \text{ mm}^2$ ). It can generate more than 4000 stimulating spots on the retina, where each spot can stimulate a single neuron with the required temporal resolution. We tested the capacity of the photonic matrix to generate action potentials in retinas of *rd1* mice with ChR2 expressed in the retinal ganglion cells (RGCs). The *rd1* mice lose their photoreceptors by 4 weeks of age [74]. Thus, at 4–5 weeks after birth, the right eyes of the mice were injected with pAAV-double

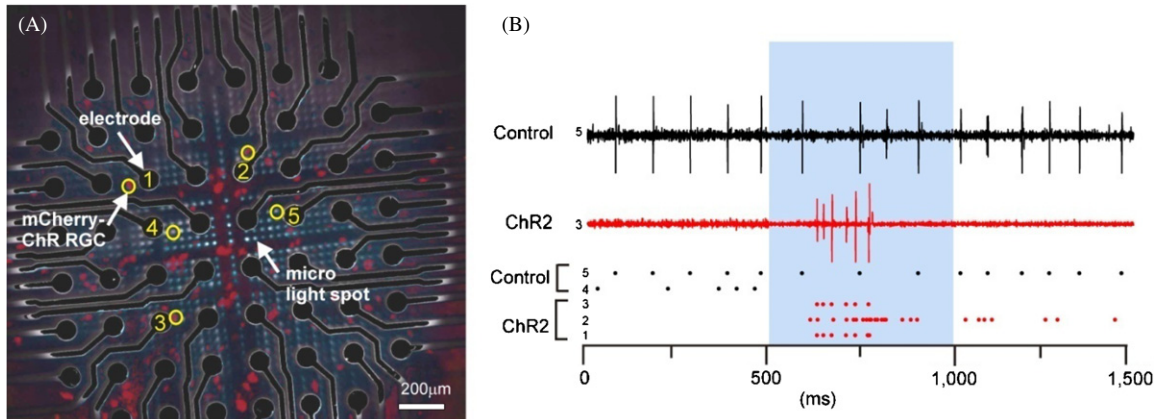


**Figure 8.** Stimulation of ChR2-expressing *rd1* retina. (A) Image of the whole micro-LEDs projected 1:1 on ChR2-expressing isolated retina of *rd1* mouse that was placed on a flat MEA60 (an overlaid image of brightfield micro-LED illumination and a fluorescence imaging of the mCherry tag). Stimulation sites are circled and recorded electrodes are labelled in yellow. (B) Example of light-evoked spike trains induced by spots (circled) near electrodes 1:5. Control, non-transfected RGC; ChR2, transfected RGCs; spots 1:3 cover ChR2 expressing RGCs; spots 4:5 cover non-transfected RGCs. Spikes (dots) recorded from multiple cells are illustrated by raster plots.

floxed-hChR2(H134R)-mCherry-WPRE-pA (see section 2). Isolated ChR2-transfected retinas were placed on a flat 60-channel MEA (Multichannel Systems) that was placed on the stage of a microscope. Figure 8 shows the micro-LEDs imaged on the *rd1* retina in which some of the RGCs express ChR2 (visualized by the red fluorescent tag of the mCherry). When ChR2-expressing RGCs were illuminated by the micro-spots of light, they generated trains of action potentials, as seen in figure 8. RGCs that did not express ChR2 had no activity that was time locked with the light stimulus. In this experiment, the micro-LEDs illuminated came from the bottom, i.e. directly on the RGCs layer, and hence the stimulating light was not significantly scattered. Moreover, retina has relative low scattering coefficient of  $12 \text{ mm}^{-1}$  [75], i.e. the light irradiance drops by half after  $80 \mu\text{m}$ . However, applying the micro-LEDs to brain tissue will involve much larger scattering which can vary depending on species and physiological status of the tissue [76]. Thus, applying the micro-LEDs to tissue will be affected by the scattering that will determine the axial penetration and the lateral resolution.

#### 4. Discussion

We described setups for neural network stimulation and for single-cell computation studies. The neural network setup images the micro-LEDs 1:1 resulting in a large  $3 \times 3 \text{ mm}^2$  illumination field, in which a single light spot has  $30 \mu\text{m}$  FWHM and up to  $3 \text{ mW mm}^{-2}$  irradiance. The single-cell setup de-magnifies the micro-LEDs 10:1, resulting in a small  $0.3 \times 0.3 \text{ mm}^2$  field, in which a single light spot has  $3 \mu\text{m}$  FWHM and up to  $300 \text{ mW mm}^{-2}$  irradiance. Both setups generate illuminations on a fixed grid with dim gaps between spots (fill factor  $\sim 16\%$ ). In the case of the 1:1 imaging, the dim gap between spots is  $20 \mu\text{m}$  and can limit the choice of neuronal targets, which may be critical for experiments such as circuit mapping. In these cases, the 10:1 imaging setup can be used since it generates illumination with only  $2 \mu\text{m}$  gaps between spots. However, the limiting

factor with the 10:1 setup is the small field of illumination ( $0.3 \times 0.3 \text{ mm}^2$ ). Alternatively, a denser array can be made—GaN LEDs can be fabricated with a diameter less than  $10 \mu\text{m}$  and hexagonal grid structure can be used to increase the fill factor. At present, however, the inter LED spacing is limited by the bonding process to the chip which requires minimum interconnection pitches of  $50\text{--}100 \mu\text{m}$  [8]. The fill factor of the illumination can be improved as well by integrating arrays of micro-lenses on top of the micro-LEDs that collimate the light, as was previously shown [77]. Integration of micro-lenses has additional advantages. First, it enables reduction of the dimensions of the emitters and thus improves the thermal performances of the chip and hence its efficiency and power consumption. Second, it can eliminate the need for additional optics and hence miniaturize the setup. Both of these considerations will be important for neural prosthesis applications.

The micro-LED array presented in this paper was driven in a matrix addressing approach. This approach has the advantage of reducing the control lines to  $2N$  (instead of  $N^2$ ); however, activation of multiple rows can lead to illumination cross-talk (i.e. activation of non-desired LEDs). For example, pulsing emitters r2/c3 (row 2 and column 3) and r3/c2 results in undesired activation of emitters r2/c2 and r3/c3. This issue can be avoided by raster scanning between the required rows. The fast clock of the peripheral interface controller enables scanning with temporal resolution of  $40 \mu\text{s}$  per row. Nevertheless, raster scanning between a large number of rows will significantly reduce the effective emission power per emitter and introduce a delay between emitters, which is proportional to the number of rows. For example, raster scanning of 64 rows will reduce the effective emission of a single micro-LED by  $1/64$  and will introduce delay of  $>2.5 \text{ ms}$  between the first and last row. This problem can be solved by integrating a flip-chip-bonded CMOS control chip to provide each LED with independent control, as has been shown by Rae *et al* [78].

The temporal resolution presented here was limited to 20 Hz, because at higher frequencies the fidelity of the

stimulation decreased and spikes were not elicited reliably. The temporal resolution is limited by the photo-cycle kinetics of ChR2 and hence is the same for any light source. Nevertheless, since the strength of ChR2-evoked depolarization depends on the light irradiance and on the level of ChR2 expression in the cells (the stronger the excitation light and the higher the expression of ChR2 in the neuron, the larger the evoked currents), the actual achievable resolution can vary between illumination systems and neuronal models (indeed 50 Hz spiking was reported by others [56]). This intrinsic limitation of ChR2 may be a disadvantage in comparison to electrical stimulation techniques. However, since the mean spiking frequency of neural networks as well as many important phenomena, such as oscillation, is smaller than 50 Hz [79], it might be sufficient for most neural network studies.

Recently, nematic liquid-crystal spatial light modulators (LC-SLMs) were used to generate single photon [80] and two-photon [81] photolysis patterns of caged glutamate. LC-SLMs can modulate the wave front (phase) of a laser beam by displaying a Fourier transform of the required illumination pattern. Such an approach has a unique capacity for spot shaping, two-photon excitation and even limited axial control. Nevertheless, its temporal resolution is fundamentally limited by the slow (>10 ms) reorientation time of the liquid crystals and by the calculation time of the Fourier planes (it typically requires several iterations, but can be pre-computed in non-real-time applications). As such, it can be difficult to generate individual spike patterns in different neuronal targets regardless of the photosensitization technique (ChR2 or caged glutamate), for example, stimulating two neurons with a 1 ms delay. Ferroelectric LCs can provide fast (up to 1 kHz) refresh rate; however, in these binary modulators, the efficiency of the modulation is limited to 40% and their addressable field is smaller [82]. Spatial light modulators based on digital micro-mirror devices (DMDs) [83] have also been proposed, as the micro-mirrors can be switched at high frequencies (several kHz). Their use for patterned photostimulation was recently demonstrated on light-activated ionotropic glutamate receptors [84] and was suggested for ChR2 [52]. Nowadays, research versions of DMD, which allow for better control than proprietary systems, have become available. However, a key drawback of the DMDs (as with LCD systems) is that a large fraction of light power is always lost since the patterning is created by redirecting unwanted light out of the excitation field. This is a severe disadvantage for portable and neural prosthetic applications [82], which cannot use bulky cooling systems and require battery power. In addition, the maximum power which can be transmitted through them may be limited as absorption will cause local heating and melting of the mirror.

The photonic matrix we describe in this work is a multi-light source device and hence fundamentally different from LC-SLM and DMD that modulate the light from a single beam. There are advantages and disadvantages to each approach. In comparison to SLM, the micro-LED matrix we present here has a smaller fill factor and is limited to a fixed grid thus has a smaller coverage of the neural sample. However, it has the advantage that individual light spots can operate independently

with almost nanosecond resolution [85]. In addition, the photonic matrix is a compact and simple to operate solution that can be easily adopted by researchers and can present a powerful solution for neural prosthesis applications.

## 5. Conclusions

We presented a development and a proof-of-concept of a novel two-dimensional photostimulation tool that is based on a matrix of  $64 \times 64$  high-power micro-LEDs. We described setups for neural network stimulation and for single-cell computation studies. We demonstrated that even the low irradiance spots have sufficient power to elicit precisely timed action potentials and dendritic currents in ChR2-expressing neurons and showed examples of potential applications for the technology. The matrix photostimulation is a simple and powerful tool that can provide sophisticated spatiotemporal stimulation patterns for studying neural network dynamics, neuronal disorders and for neural prosthesis applications.

## Acknowledgments

This work was funded by the UK Engineering Physical Sciences Research Council (F029241), the UK Biological and Biotechnology Research Council (F021127) and the University of London Central Research. The development of the micro-LED array was funded by the RCUK Basic Technology Research Programme (GR/S85764/1). NG acknowledges the support of the Kenneth Lindsay Foundation and KN acknowledges the support of the Wilfred Corrigan Foundation. The authors would like to thank Boton Roska and David Balya (FMI, Basel) for their help with the *rd1* mice experiments and Karl Deisseroth for the ChR2 vectors.

## References

- [1] Varela F, Lachaux J P, Rodriguez E and Martinerie J 2001 The brainweb: phase synchronization and large-scale integration *Nat. Rev.* **2** 229–39
- [2] Uhlhaas P J and Singer W 2006 Neural synchrony in brain disorders: relevance for cognitive dysfunctions and pathophysiology *Neuron* **52** 155–68
- [3] Thomas C A Jr, Springer P A, Loeb G E, Berwald-Netter Y and Okun L M 1972 A miniature microelectrode array to monitor the bioelectric activity of cultured cells *Exp. Cell Res.* **74** 61–6
- [4] Hofmann F and Bading H 2006 Long term recordings with microelectrode arrays: studies of transcription-dependent neuronal plasticity and axonal regeneration *J. Physiol. (Paris)* **99** 125–32
- [5] Lante F, de Jesus Ferreira M C, Guiramand J, Recasens M and Vignes M 2006 Low-frequency stimulation induces a new form of LTP, metabotropic glutamate (mGlu5) receptor- and PKA-dependent, in the CA1 area of the rat hippocampus *Hippocampus* **16** 345–60
- [6] Cang J, Renteria R C, Kaneko M, Liu X, Copenhagen D R and Stryker M P 2005 Development of precise maps in visual cortex requires patterned spontaneous activity in the retina *Neuron* **48** 797–809
- [7] Aton S J, Colwell C S, Hattar A J, Waschek J and Herzog E D 2005 Vasoactive intestinal polypeptide mediates circadian rhythmicity and synchrony in mammalian clock neurons *Nat. Neurosci.* **8** 476–83

- [8] Degenaar P, Grossman N, Memon M A, Burrone J, Dawson M, Drakakis E, Neil M and Nikolic K 2009 Optobionic vision—a new genetically enhanced light on retinal prosthesis *J. Neural Eng.* **6** 035007
- [9] Stuart G J and Hausser M 2001 Dendritic coincidence detection of EPSPs and action potentials *Nat. Neurosci.* **4** 63–71
- [10] Neves G, Cooke S F and Bliss T V 2008 Synaptic plasticity, memory and the hippocampus: a neural network approach to causality *Nat. Rev.* **9** 65–75
- [11] Waters J, Schaefer A and Sakmann B 2005 Backpropagating action potentials in neurones: measurement, mechanisms and potential functions *Prog. Biophys. Mol. Biol.* **87** 145–70
- [12] Golding N L and Spruston N 1998 Dendritic sodium spikes are variable triggers of axonal action potentials in hippocampal CA1 pyramidal neurons *Neuron* **21** 1189–200
- [13] Gradinaru V, Thompson K R, Zhang F, Mogri M, Kay K, Schneider M B and Deisseroth K 2007 Targeting and readout strategies for fast optical neural control *in vitro* and *in vivo* *J. Neurosci.* **27** 14231–8
- [14] Schoenenberger P, Grunditz A, Rose T and Oertner T G 2008 Optimizing the spatial resolution of Channelrhodopsin-2 activation *Brain Cell Biol.* **36** 119–27
- [15] Fork R L 1971 Laser stimulation of nerve cells in aplysia *Science* **171** 907–8
- [16] Izzo A D, Walsh J T Jr, Ralph H, Webb J, Bendett M, Wells J and Richter C P 2008 Laser stimulation of auditory neurons: effect of shorter pulse duration and penetration depth *Biophys. J.* **94** 3159–66
- [17] Messenger J, Katayama Y, Ogden D, Corrie J and Trentham D 1991 Photolytic release of glutamate from caged glutamate expands squid chromatophores *J. Physiol., Lond.* **438** 293P
- [18] Shoham S, O'Connor D H, Sarkisov D V and Wang S S 2005 Rapid neurotransmitter uncaging in spatially defined patterns *Nat. Methods* **2** 837–43
- [19] Yoshimura Y, Dantzer J L and Callaway E M 2005 Excitatory cortical neurons form fine-scale functional networks *Nature* **433** 868–73
- [20] Miesenböck G and Kevrekidis I G 2005 Optical imaging and control of genetically designated neurons in functioning circuits *Ann. Rev. Neurosci.* **28** 533–63
- [21] Pettit D L, Wang S S, Gee K R and Augustine G J 1997 Chemical two-photon uncaging: a novel approach to mapping glutamate receptors *Neuron* **19** 465–71
- [22] Volgraf M, Gorostiza P, Numano R, Kramer R H, Isacoff E Y and Trauner D 2006 Allosteric control of an ionotropic glutamate receptor with an optical switch *Nat. Chem. Biol.* **2** 47–52
- [23] Szobota S *et al* 2007 Remote control of neuronal activity with a light-gated glutamate receptor *Neuron* **54** 535–45
- [24] Gentile M, Latonen L and Laiho M 2003 Cell cycle arrest and apoptosis provoked by UV radiation-induced DNA damage are transcriptionally highly divergent responses *Nucleic Acids Res.* **31** 4779–90
- [25] Nagel G, Szellas T, Huhn W, Kateriya S, Adeishvili N, Berthold P, Ollig D, Hegemann P and Bamberg E 2003 Channelrhodopsin-2, a directly light-gated cation-selective membrane channel *Proc. Natl Acad Sci USA* **100** 13940–5
- [26] Schobert B and Lanyi J K 1982 Halorhodopsin is a light-driven chloride pump *J. Biol. Chem.* **257** 10306–13
- [27] Feldbauer K, Zimmermann D, Pintschovius V, Spitz J, Bamann C and Bamberg E 2009 Channelrhodopsin-2 is a leaky proton pump *Proc. Natl Acad Sci USA* **106** 12317–22
- [28] Boyden E S, Zhang F, Bamberg E, Nagel G and Deisseroth K 2005 Millisecond-timescale, genetically targeted optical control of neural activity *Nat. Neurosci.* **8** 1263–8
- [29] Li X, Gutierrez D V, Hanson M G, Han J, Mark M D, Chiel H, Hegemann P, Landmesser L T and Herlitze S 2005 Fast noninvasive activation and inhibition of neural and network activity by vertebrate rhodopsin and green algae channelrhodopsin *Proc. Natl Acad Sci USA* **102** 17816–21
- [30] Ishizuka T, Kakuda M, Araki R and Yawo H 2006 Kinetic evaluation of photosensitivity in genetically engineered neurons expressing green algae light-gated channels *Neurosci. Res.* **54** 85–94
- [31] Petreanu L, Huber D, Sobczyk A and Svoboda K 2007 Channelrhodopsin-2-assisted circuit mapping of long-range callosal projections *Nat. Neurosci.* **10** 663–8
- [32] Zhang Y P and Oertner T G 2007 Optical induction of synaptic plasticity using a light-sensitive channel *Nat. Methods* **4** 139–41
- [33] Zhang Y P, Holbro N and Oertner T G 2008 Optical induction of plasticity at single synapses reveals input-specific accumulation of alphaCaMKII *Proc. Natl Acad Sci USA* **105** 12039–44
- [34] Liewald J F, Brauner M, Stephens G J, Bouhours M, Schultheis C, Zhen M and Gottschalk A 2008 Optogenetic analysis of synaptic function *Nat. Methods* **5** 895–902
- [35] Nagel G, Brauner M, Liewald J F, Adeishvili N, Bamberg E and Gottschalk A 2005 Light activation of channelrhodopsin-2 in excitable cells of *Caenorhabditis elegans* triggers rapid behavioral responses *Curr. Biol.* **15** 2279–84
- [36] Petreanu L, Mao T, Sternson S M and Svoboda K 2009 The subcellular organization of neocortical excitatory connections *Nature* **457** 1142–5
- [37] Hira R, Honkura N, Noguchi J, Maruyama Y, Augustine G J, Kasai H and Matsuzaki M 2009 Transcranial optogenetic stimulation for functional mapping of the motor cortex *J. Neurosci. Methods* **179** 258–63
- [38] Gradinaru V, Mogri M, Thompson K R, Henderson J M and Deisseroth K 2009 Optical deconstruction of parkinsonian neural circuitry *Science* **324** 354–9
- [39] Ayling O G, Harrison T C, Boyd J D, Goroshkov A and Murphy T H 2009 Automated light-based mapping of motor cortex by photoactivation of channelrhodopsin-2 transgenic mice *Nat. Methods* **6** 219–24
- [40] Lagali P S, Balya D, Awatramani G B, Munch T A, Kim D S, Busskamp V, Cepko C L and Roska B 2008 Light-activated channels targeted to ON bipolar cells restore visual function in retinal degeneration *Nat. Neurosci.* **11** 667–75
- [41] Huber D, Petreanu L, Ghitanu N, Ranade S, Hromadka T, Mainen Z and Svoboda K 2008 Sparse optical microstimulation in barrel cortex drives learned behaviour in freely moving mice *Nature* **451** 61–4
- [42] Wang H *et al* 2007 High-speed mapping of synaptic connectivity using photostimulation in channelrhodopsin-2 transgenic mice *Proc. Natl Acad Sci USA* **104** 8143–8
- [43] Arenkiel B R, Peca J, Davison I G, Feliciano C, Deisseroth K, Augustine G J, Ehlers M D and Feng G 2007 *In vivo* light-induced activation of neural circuitry in transgenic mice expressing channelrhodopsin-2 *Neuron* **54** 205–18
- [44] Adamantidis A R, Zhang F, Aravanis A M, Deisseroth K and de Lecea L 2007 Neural substrates of awakening probed with optogenetic control of hypocretin neurons *Nature* **450** 420–4
- [45] Bi A, Cui J, Ma Y P, Olshevskaya E, Pu M, Dizhoor A M and Pan Z H 2006 Ectopic expression of a microbial-type rhodopsin restores visual responses in mice with photoreceptor degeneration *Neuron* **50** 23–33
- [46] Pulver S R, Pashkovski S L, Hornstein N J, Garrity P A and Griffith L C 2009 Temporal dynamics of neuronal activation by channelrhodopsin-2 and TRPA1 determine behavioral output in *Drosophila* larvae *J. Neurophysiol.* **101** 3075–88

- [47] Borue X, Cooper S, Hirsh J, Condrion B and Venton B J 2009 Quantitative evaluation of serotonin release and clearance in *Drosophila* *J. Neurosci. Methods* **179** 300–8
- [48] Zhang W, Ge W and Wang Z 2007 A toolbox for light control of *Drosophila* behaviors through channelrhodopsin 2-mediated photoactivation of targeted neurons *Eur. J. Neurosci.* **26** 2405–16
- [49] Schroll C *et al* 2006 Light-induced activation of distinct modulatory neurons triggers appetitive or aversive learning in *Drosophila* larvae *Curr. Biol.* **16** 1741–7
- [50] Abbott S B, Stornetta R L, Fortuna M G, Depuy S D, West G H, Harris T E and Guyenet P G 2009 Photostimulation of retrotrapezoid nucleus phox2b-expressing neurons *in vivo* produces long-lasting activation of breathing in rats *J. Neurosci.* **29** 5806–19
- [51] Alilain W J, Li X, Horn K P, Dhingra R, Dick T E, Herlitze S and Silver J 2008 Light-induced rescue of breathing after spinal cord injury *J. Neurosci.* **28** 11862–70
- [52] Farah N, Reutsky I and Shoham S 2007 Patterned optical activation of retinal ganglion cells *Conf. Proc. IEEE Eng. Med. Biol. Soc.* **2007** 6369–71
- [53] Han X, Qian X, Bernstein J G, Zhou H H, Franzesi G T, Stern P, Bronson R T, Graybiel A M, Desimone R and Boyden E S 2009 Millisecond-timescale optical control of neural dynamics in the nonhuman primate brain *Neuron* **62** 191–8
- [54] Degenaar P 2009 Elucidating the nervous system with channelrhodopsins *Cell Sci. Rev.* **6** (available at [www.cellscience.com/Reviews21/Channelrhodopsins\\_CNS.html](http://www.cellscience.com/Reviews21/Channelrhodopsins_CNS.html))
- [55] Zhang F, Wang L P, Boyden E S and Deisseroth K 2006 Channelrhodopsin-2 and optical control of excitable cells *Nat. Methods* **3** 785–92
- [56] Aravanis A M, Wang L P, Zhang F, Meltzer L A, Mogri M Z, Schneider M B and Deisseroth K 2007 An optical neural interface: *in vivo* control of rodent motor cortex with integrated fiberoptic and optogenetic technology *J. Neural Eng.* **4** S143–56
- [57] Campagnola L, Wang H and Zylka M J 2008 Fiber-coupled light-emitting diode for localized photostimulation of neurons expressing channelrhodopsin-2 *J. Neurosci. Methods* **169** 27–33
- [58] Bernstein J G, Han X, Henninger M A, Ko E Y, Qian X, Franzesi G T, McConnell J P, Stern P, Desimone R and Boyden E S 2008 Prosthetic systems for therapeutic optical activation and silencing of genetically-targeted neurons *Proc. Soc. Photo-Opt. Instrum. Eng.* **6854** 68540H
- [59] Gobel W, Kampa B M and Helmchen F 2007 Imaging cellular network dynamics in three dimensions using fast 3D laser scanning *Nat. Methods* **4** 73–9
- [60] Nikolenko V, Poskanzer K E and Yuste R 2007 Two-photon photostimulation and imaging of neural circuits *Nat. Methods* **4** 943–50
- [61] Poher V *et al* 2008 Micro-LED arrays: a tool for two-dimensional neuron stimulation *J. Phys. D: Appl. Phys.* **41** 9
- [62] Jeon C W, Kim K S and Dawson M D 2002 Fabrication of two-dimensional InGaN-based micro-LED arrays *Phys. Status Solidi a* **192** 325–8
- [63] Choi H W, Jeon C W and Dawson M D 2004 Fabrication of matrix-addressable micro-LED arrays based on a novel etch technique *J. Cryst. Growth* **268** 527–30
- [64] Laia Y L, Liua C P and Chenb Z Q 2005 InGaN/GaN superlattices from blue, green to yellow by controlling the size of InGaN quasi-quantum dot *Thin Solid Films* **498** 128–32
- [65] Strite S and Morkoc H 1992 GaN, AlN, and InN: a review *J. Vac. Sci. Technol.* **10** 1237
- [66] Gong Z, Zhang H X, Gu E, Griffin C, Dawson M D, Poher V, Kennedy G T, French P M W and Neil M A A 2007 Matrix-addressable micropixelated InGaN light-emitting diodes with uniform emission and increased light output *IEEE Trans. Electron Devices* **54** 8
- [67] Köhler A 1893 Gedanken zu einem neuen Beleuchtungsverfahren für mikrophotographische Zwecke *Zeitschrift für Wissenschaftliche Mikroskopie*
- [68] Brewer G J, Boehler M D, Ide A N and Wheeler B C 2009 Chronic electrical stimulation of cultured hippocampal networks increases spontaneous spike rates *J. Neurosci. Methods* **184** 104–9
- [69] Abbott L F 1999 Lopicque's introduction of the integrate-and-fire model neuron (1907) *Brain Res. Bull.* **50** 303–4
- [70] Rinzel J and Rall W 1974 Transient response in a dendritic neuron model for current injected at one branch *Biophys. J.* **14** 759–90
- [71] Ascoli G A 2006 Mobilizing the base of neuroscience data: the case of neuronal morphologies *Nat. Rev. Neurosci.* **7** 318–24
- [72] Sommerhalder J 2008 Visual prostheses research *ARVO Ann. Meeting Exp. Rev. Ophthalmol.* **3** 389–91
- [73] Weiland J D and Humayun M S 2008 Visual prosthesis *Proc. IEEE* **96** 1076–84
- [74] Farber D B, Flannery J G and Bowes-Rickman C 1994 The rd mouse story: seventy years of research on an animal model of inherited retinal degeneration *Prog. Retin. Eye Res.* **13** 31–64
- [75] Hammer H, Schweitzer D, Thamm E, Kolb A and Strobel J 2001 Scattering properties of the retina and the choroids determined from OCT-A-scans *Int. Ophthalmol.* **23** 291–5
- [76] Yaroslavsky A N, Schulze P C, Yaroslavsky I V, Schober R, Ulrich F and Schwarzaier H J 2002 Optical properties of selected native and coagulated human brain tissues *in vitro* in the visible and near infrared spectral range *Phys. Med. Biol.* **47** 2059–73
- [77] Choi H W, Gu E, Liu C, Girkin J M and Dawson M D 2005 Fabrication and evaluation of GaN negative and bifocal microlenses *J. Appl. Phys.* **97** 063101
- [78] Rae B R, Griffin C, McKendry J, Girkin J M, Zhang H X, Gu E, Renshaw D, Charbon E, Dawson M D and Henderson R K 2008 CMOS driven micro-pixel LEDs integrated with single photon avalanche diodes for time resolved fluorescence measurements *J. Phys. D: Appl. Phys.* **41** 094011
- [79] Vogels T P, Rajan K and Abbott L F 2005 Neural network dynamics *Ann. Rev. Neurosci.* **28** 357–76
- [80] Lutz C, Otis T S, DeSars V, Charpak S, DiGregorio D A and Emiliani V 2008 Holographic photolysis of caged neurotransmitters *Nat. Methods.* **5** 821–7
- [81] Nikolenko V, Watson B O, Araya R, Woodruff A, Peterka D S and Yuste R 2008 SLM microscopy: scanless two-photon imaging and photostimulation with spatial light modulators *Front. Neural Circuits* **2** 5
- [82] Golan L, Reutsky I, Farah N and Shoham S 2009 Design and characteristics of holographic neural photo-stimulation systems *J. Neural Eng.* **6** 66004
- [83] Hornbeck L J 1991 Spatial light modulator and method *US* 5061049
- [84] Wang S, Szobota S, Wang Y, Volgraf M, Liu Z, Sun C, Trauner D, Isacoff E Y and Zhang X 2007 All optical interface for parallel, remote, and spatiotemporal control of neuronal activity *Nano Lett.* **7** 3859–63
- [85] Zhang H X, Massoubre D, McKendry J, Gong Z, Guilhabert B, Griffin C, Gu E, Jessop P E, Girkin J M and Dawson M D 2008 Individually-addressable flip-chip AlInGaN micropixelated light emitting diode arrays with high continuous and nanosecond output power *Opt. Express* **16** 9918–26